Communication

The Influence of Nanoparticles of Graphene Oxide-PEG on Cytokine Profile of Monocytes from Human Blood In Vitro

Usanina D.I. [1,2*] , Bochkova M.S. [1,2] , Timganova V.P. [1] , Shardina K. Yu. [1] , Zamorina S.A. [1,2] , Rayev M.B. [1,2]

[1] Branch of the Perm Federal Research Center, Ural Branch of the Russian Academy of Sciences, Institute of Ecology and Genetics of Microorganisms, Perm 614081, Russia

[2] Department of Microbiology and Immunology, Faculty of Biology, Perm State National Research University, Perm 614068, Russia

[*] Correspondence: usanina_d@mail.ru

Abstract: This study investigated the response of human monocytes to co-culture with pegylated (linear or branched) graphene oxide (GO) nanoparticles, specifically examing both small (P-GOs, 100 -200 nm) and larger (P-GOb, 1-5 μm) particles at concentrations of 5, 25, and 50 μg mL^{-1}. Human monocytes (CD14$^+$ cells) were isolated and cultured with these nanoparticles for 72 hours. We measured cell viability, lactate dehydrogenase (LDH) release, and cytokine production. The findings showed that P-GO nanoparticles had little effect on cytokine production, including MIF, GM-CSF, VEGF, IP-10, IL-8, HGF, and SCGF-beta in vitro. At a low concentration (5 μg mL^{-1}), P-GO exhibited minimal influence on cytokines, except forthe LP-GOb variant, which increased M-CSF production. Conversely, 25 and 50 μg mL^{-1} of P-GO nanoparticles enhanced the release of variouscytokines, including proinflammatory IL-6, IL-1β, IL-1α, IL-18, IL-17, IL-16, IFN-γ, TNF-β, TNF-α, anti-inflammatory IL-1ra, IL-13, IL-10, IL-4, regulatory G-CSF, IL-2, IL-3, IL-5, IL-12 (p40), IL-12 (p70), M-CSF, GM-CSF and chemokines CTACK, Eotaxin, GRO-α, RANTES, MIP-1β, MCP-1, MIP-1α, MCP-3, MIG, SDF-1α, growth factors Basic FGF, PDGF-BB, SCF, and LIF and TRAIL. Although higher concentrations of P-GO nanoparticles resulted in significant cytokine production, monocyte viability remained largely unaffected . LDH release was elevated solely in samples treated with 50 μg mL^{-1} of LP-GOb. BP-GOs showed minimal influence on cytokine profiles, raising M-CSF levels at the highest concentration. These results indicate that modifying graphene oxide nanoparticles may hold potential for creating graphene-based pharmacological agents.

Keywords: PEG; Graphene Oxide Nanoparticles; Monocyte; Cytokine; Chemokine; Growth Factor

1. Introduction

The need for developing therapeutic agents, treatment methods, diagnostic techniques, and more drives scientific exploration across various fields. One promising area of research is the search for and application of different materials, particularly carbon nanomaterials [1]. Graphene is a fascinating carbon material. This two-dimensional substance boasts unique electronic and conductive properties thanks to its distinctive structure. Graphene, in its original unoxidized form, is a hydrophobic substance that tends to aggregate [2]. The most extensively studied

graphene derivative is graphene oxide (GO), which exhibits better stability in colloidal solution and is easier to functionalize due to its oxygen-containing functional groups [3]. Graphene oxide is a promising material for drug delivery systems, particularly for antitumor drugs, due to its two-dimensional aromatic surface. This unique structure allows GO to act as a substrate, facilitating the adsorption and delivery of drugs. When drugs are loaded onto GO, they form stable complexes, enhancing the efficiency of drug delivery mechanisms [4]. The small thickness of graphene, just one atom, combined with its exceptional conductivity, makes it an ideal material for developing a variety of biomedical sensors. These sensors include enzyme biosensors, immunosensors, and DNA sensors [5]. When functionalized with dyes, polymers, nanoparticles, drugs, and biomolecules, graphene oxide becomes a versatile platform for various bioimaging applications [6].

Graphene oxide has emerged as a highly adaptable nanomaterial for therapeutic applications, especially in the realm of cancer treatment. GO demonstrates remarkable photothermal conversion capabilities when subjected to near-infrared (NIR) light. This characteristic enables its use in photothermal therapy (PTT), where it generates heat upon irradiation, resulting in targeted destruction of tumors [7]. The synergy between GO and photothermal agents enhances the efficacy of cancer therapies by elevating the temperature at the tumor site, which promotes apoptosis in cancer cells [8]. Additionally, in photodynamic therapy (PDT), GO can facilitate the delivery of photosensitizers that produce reactive oxygen species when activated by light. This process effectively induces cell death in cancerous cells while protecting adjacent healthy tissues. The combination of GO with PDT presents a promising strategy for treating various tumor types [7].

The potential applications of graphene oxide are vast and diverse, making it an exciting material in numerous fields. However, the use of nanomaterials in living systems such as the human body raises significant safety concerns. The immune system is essential in determining how nanomaterials interact with living organisms, including humans. Grasping this interaction is critical for the secure and efficient application of nanotechnology in the field of medicine. Graphene oxide, being a non-biodegradable material, will persist in the body for a prolonged duration [9]. Phagocytes, among which macrophages and monocytes, are typically the first cells of the immune system to come into contact with nanoparticles within the body [10]. Therefore, immunotoxicity studies tend to focus on these cell types.

A considerable amount of research indicates that the immune-modulating effects of graphene oxide are significantly influenced by various characteristics of the material. These factors comprise concentration, shape, size, type of functionalization, as well as the method of administration and exposure time [11]. Research indicates that covering nanoparticle surfaces with biocompatible polymers, particularly polyethylene glycol (PEG), can significantly reduce their potential cytotoxicity [12].

We have previously assessed the effect of PEG-coated graphene oxide on the functions and metabolism of human monocytes; however, the cytokine profile has not yet been investigated [13, 14]. Studies suggest that carbon nanomaterials frequently result in heightened production of inflammatory cytokines by immune system cells [15–18]. In light of this, the objective of the present study is to examine the impact of PEGylated graphene oxide on the cytokine profile of monocytes in vitro.

2. Materials and Methods

2.1. Donors

The research was carried out in compliance with the WMA Declaration of Helsinki 2000 and the Protocol of the Council of Europe Convention on Human Rights and Biomedicine 1999. Approval for the experimental design was obtained from the Ethics Committee of the IEGM Ural Branch of the Russian Academy of Sciences (IRB00010009) on August 30, 2019. Written informed consent was obtained from all participants. The authors complied with all applicable ethical standards.

2.2. Cell Isolation

We collected peripheral blood from healthy donors (n = 4, aged 22 ± 2 years). Mononuclears (PBMC) were separated from heparinized blood through density gradient centrifugation using Diacoll (ρ = 1.077) (DiaM, Russia). After centrifuging the PBMCs located above the Diacoll layer were harvested, diluted with RPMI-1640 medium, and centrifuged three times in RPMI-1640. The resulting cell sediment was then resuspended, and the concentration

of PBMCs was determined in a Neubauer hemocytometer.

Then we isolated CD14$^+$ cells (monocytes) from the PBMCs using magnetic microbeads, columns, and stand (Miltenyi Biotec, Germany). The percentage of CD14$^+$ monocytes was 96.4%.

Monocytes were incubated with P-GO nanoparticles (5, 25, 50 µg mL^{-1}) for 72 h. Cells were cultured in RPMI-1640 medium (Gibco, USA) supplemented with 2 mM L-glutamine, 100 U penicillin, 0.1 mg mL^{-1} streptomycin, 2.5 µg mL^{-1} amphotericin B, and 10% fetal bovine serum (FBS) (all Capricorn, Germany) in flat-bottom 96-well culture plates (SPL, South Korea). After incubation, cell viability and cytokine profile were assessed. We selected a sufficiently long cultivation period due to the limited information available in the literature, as cells are typically cultured with nanomaterials for 24 to 48 hours [19, 20].

2.3. Graphene Oxide

Graphene oxide nanoparticles with lateral dimensions of 100–200 nm (P-GOs) and 1–5 µm (P-GOb) (Ossila Ltd., UK) were utilized. These nanoparticles were functionalized with linear and branched (LP-GO and BP-GO) PEG. In the process of functionalization of graphene oxide, amino groups from PEG-NH$_2$ and 8arm-PEG-NH$_2$ were covalently attached to the GO surface carboxyl groups. The process of chemical modification and characteristics of the obtained material have been detailed in one of our previously published publications [13]. The characteristics of the P-GO nanoparticles are summarized in Figure A1 and Table A1.

2.4. Cell Viability

Monocytes (106 cells mL−1) were incubated with P-GO nanoparticles for 3 days (72 hours) in complete culture medium (RPMI-1640 (Gibco, USA) with 10% FCS, 2 mM L-glutamine (ICN Pharmaceuticals, USA), and penicillin-streptomycin-amphotericin B (BI, Israel)) at 37 °C and 5% CO$_2$ in a humid atmosphere. Subsequently, the viability of cells was assessed using Erythrosine B (Logos Biosystems, South Korea) DET (dye exclusion test).

2.5. Lactate Dehydrogenase

Activity of LDH was measured using an assay kit (LDH-UF-Novo, Vector-Best, Russia) on a Multiskan Sky (Thermo Fisher Scientific, USA) spectrophotometer.

2.6. Cytokine Profile Evaluation

The levels of various cytokines and chemokines in pre-defrosted culture supernatants were measured using Bio-Plex Pro Human Cytokine Screening Panel, 48-Plex #12007283 (Bio-Rad, USA), MAGPIX® Multiplexing System (Merck Millipore, USA), and xPONENT® software. Standard curves were created using a 5PL analysis method. Data processing was performed with Belysa® Immunoassay Curve Fitting Software.

2.7. Statistical Data Analysis

Statistical data analysis was carried out using GraphPad Prism 8.0.1 software, employing the one-way ANOVA (Friedman test) and Dunn test for multiple comparisons. Results are displayed as median values along with the lower and upper quartiles. The significance threshold was established at 0.05.

3. Results

3.1. P-GO Nanoparticle Types

In this study, we used nanoparticles of four types, and their characteristics are presented in Table 1.

Table 1. P-GO nanoparticles properties.

	LP-GOs	BP-GOs	LP-GOb	BP-GOb
Size, nm	184 ± 73	287 ± 52	891 ± 18	1376 ± 48
Type of PEG	linear	branched	linear	branched

3.2. Cytotoxic Effects of P-GO

No statistically significant differences in the viability of human peripheral blood monocytes were observed between cultures with P-GO nanoparticles and those without (control) (Figure 1). We found no differences in cytotoxicity among P-GO nanoparticles of different sizes or those modified with linear or branched PEG. It is noteworthy that the median viability values were somewhat elevated in cultures with the addition of 5 μg mL^{-1} of P-GO. In contrast, a concentration of 50 μg mL^{-1} of P-GO decreased the viability of monocytes.

Overall, P-GO, according to statistical analysis, did not change the monocyte viability.
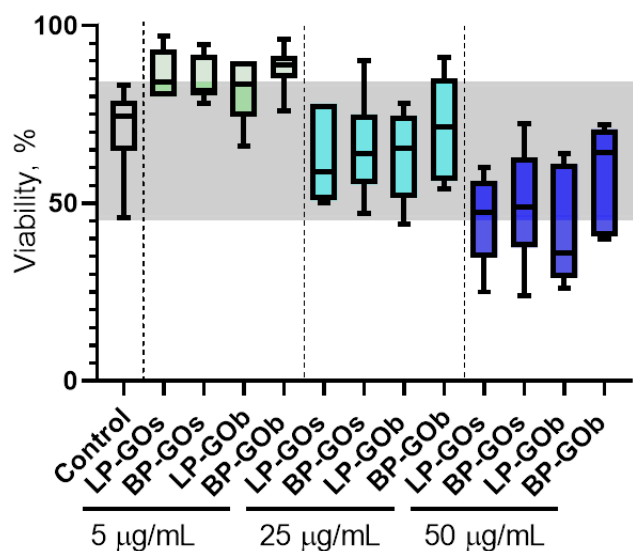

Figure 1. Viability of monocytes in cultures with P-GO nanoparticles after 72 h incubation.
Note: Medians (Me) and quartiles (Q1–Q3) are presented; n = 4.

3.3. Effect of P-GO on LDH Activity

We observed that 50 μg mL^{-1} of LP-GOb significantly elevated the release of lactate dehydrogenase (Figure 2), which can be interpreted as the rise in the number of dead cells within the monocyte culture. This finding aligns with the trend indicating an increase in the percentage of dead cells in DET.

3.4. Effect of P-GO on the Cytokine Profile of Monocytes

In the culture supernatants, several cytokines were found to be below the detection limit. Specifically, IL-5, IL-15, β-NGF, and SDF-1α were not detected in the samples. An important finding is that monocytes produced several cytokines both in the control group and when exposed to GO nanoparticles. However, the levels of these cytokines remained unchanged. The specific cytokines identified include MIF, GM-CSF, VEGF, IP-10, IL-8, HGF, and SCGF-beta.

In this study, three concentrations of GO nanoparticles were used: 5, 25 and 50 μg mL^{-1}. Consequently, it has been established that the addition of 5 μg mL^{-1} of any type of nanoparticles does not result in significant alterations to the cytokine profile, except for M-CSF. The level of this factor rises when exposed to 5 μg mL^{-1} of P-GOb particles.

Data on the effect of GO nanoparticles on cytokine production by monocytes can be found in Figure 3 and Table A2.

It was observed that raising the concentration of P-GO nanoparticles to 25 μg mL^{-1} did not alter the cytokine profile of monocytes when small-sized nanoparticles (BP-GOs) were used. In contrast, similar particles functionalized with linear PEG (LP-GOs) significantly increased the production of a broad spectrum of cytokines, including proinflammatory TNF-α, IL-1β, IFN-γ, IL-17, IL-6, IL-1α, TNF-β, IFN-α2, IL-16, anti-inflammatory IL-4, IL-1ra, IL-10, regulatory G-CSF, IL-12 (p70), IL-2, and chemokines CTACK, Eotaxin, GRO-α, MIP-1α, MCP-1, MCP-3, MIG, MIP-1β, growth factors Basic FGF, IL-7, IL-9, PDGF-BB, SCF, and LIF and TRAIL. For larger nanoparticles, LP-GOb enhanced the production of MCP-1, MCP-3, M-CSF, and MIP-1α. However, BP-GOb nanoparticles induced the production of a significantly broader range of cytokines: CTACK, Basic FGF, G-CSF, IFN-α2, IL-1α, IL-1β, IL-1ra, IL-4, IL-6, IL-7, IL-9,

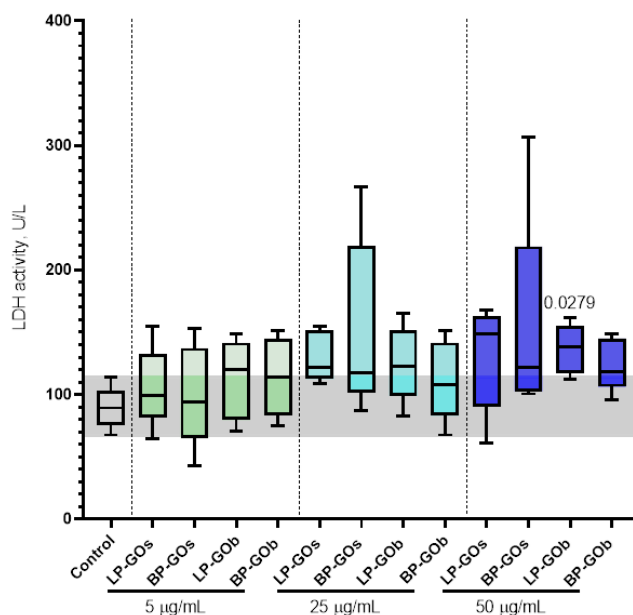IL-10, LIF, MCP-3, MIG, MIP-1α, MIP-1β, SCF, TNF-α, and TNF-β.

Figure 2. LDH activity in monocyte culture after 72 h incubation with P-GO.

Note: Medians (Me) and quartiles (Q1–Q3) are presented; n = 4. Significant differences (p < 0.05) relative to the control are noted.
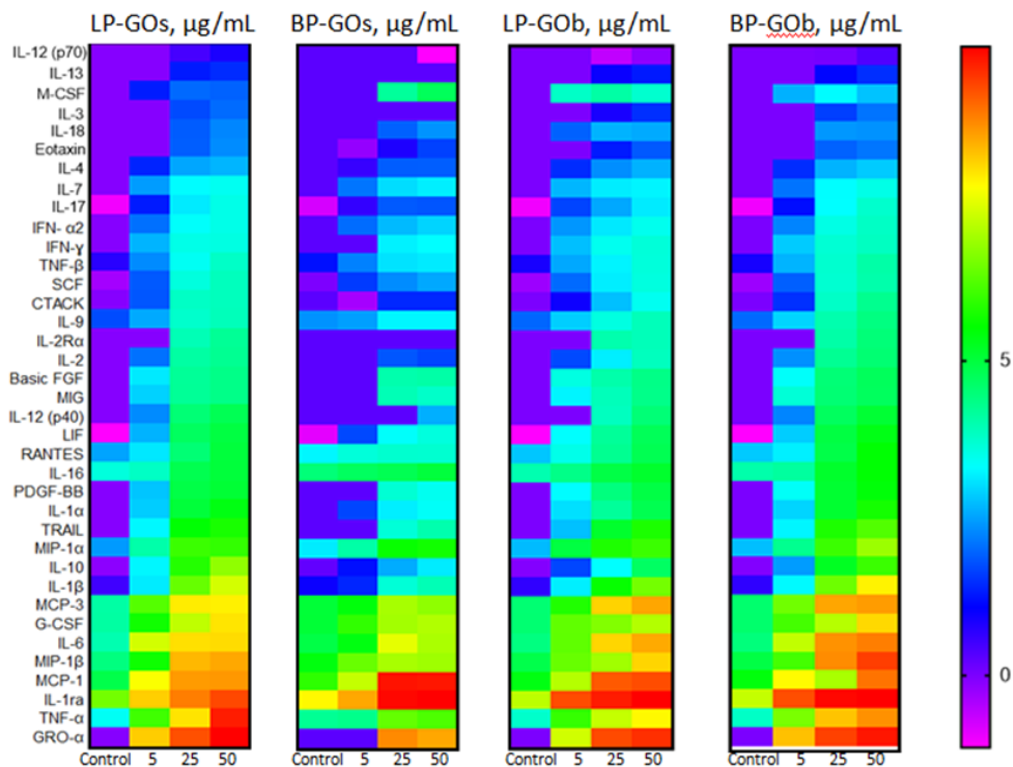
Figure 3. Effect of P-GO nanoparticles on the cytokines' concentrations in monocyte cultures.

Note: Cytokine levels shown as ln of concentrations (n = 4). IL - interleukin; M-CSF - macrophage colony-stimulating factor; IFN - interferon; TNF - tumor necrosis factor; SCF - stem cell factor; CTACK - cutaneous T cell-attracting chemokine; FGF - fibroblast growth factor; MIG - monokine induced by gamma interferon; LIF - leukemia inhibitory factor; RANTES - chemokine ligand 5 (CCL5; regulated on activation, normal T-cell expressed and secreted); PDGF-BB - platelet-derived growth factor; TRAIL - TNF-related apoptosis-inducing ligand; MIP - macrophage inflammatory protein; MCP - monocyte chemoattractant protein; G-CSF - granulocyte colony-stimulating factor; GRO - growth-related oncogene.

All types of nanoparticles at 50 μg mL^{-1} had a more pronounced influence on cytokine production by human monocytes. Small-sized nanoparticles with branched PEG (BP-GOs) induced the production of only M-CSF. In contrast, LP-GOs, stimulated the production of a wide range of regulatory molecules, including G-CSF, IL-5, IL-1β, IL-4, IL-7, IL-1α, IFN-γ, IL-10, IL-12 (p70), Eotaxin, IL-3, TNF-α, RANTES, Basic FGF, SCF, GRO-α, IL-2Rα, IL-6, LIF, MCP-1, IL-15, TRAIL, MIP-1α, CTACK, β-NGF, MIG, SDF-1α, MCP-3, MIP-1β, IL-2, IL-9, TNF-β, IL-12 (p40), IL-16, IL-17, IFN-α2, and IL-18. Larger nanoparticles coated with linear PEG (LP-GOb) also stimulated monocytes to produce CTACK and several other cytokines including Basic FGF and G-CSF. Those coated with branched PEG (BP-GOb) further enhanced the production of Eotaxin and other cytokines such as IL-2 and PDGF-BB but did not affect MCP-1 levels.

We have demonstrated that the most inert type of nanoparticles in this context are BP-GOs. All other variants of nanomaterial activated monocytes and stimulated them to produce various cytokines and chemokines, primarily pro-inflammatory ones.

When evaluating the effects of various modifications and concentrations of P-GO nanoparticles on the cytokine' production by human monocytes, it was observed that the stimulating effect becomes more pronounced with increasing nanoparticle concentration. At 5 μg mL^{-1}, there is virtually no impact on cytokine production, while 25 μg mL^{-1} induces a broader range of cytokines, which further expands at 50 μg mL^{-1}. No significant differences were found between nanoparticles of different sizes; however, surface chemistry played a crucial role. Notably, branched PEG-coated nanoparticles (BP-GOs) at concentrations of 5 and 25 μg mL^{-1} did not reliably alter cytokine production by monocytes, but at 50 μg mL^{-1}, they only increased M-CSF production. Overall, this modification of nanoparticles shows promise for developing graphene-based pharmacological agents.

For the first time, GO nanoparticles were shown to stimulate the production of CTACK, Basic FGF, GRO-α, LIF, MIG, SCF and TRAIL.

For some of the cytokines, it has also been shown not only a significant difference between individual samples compared to the control, but also differences between samples with the addition of particles that differ in one parameter (PEG type or concentration) (Table 2). No significant differences were found in the production of any cytokine depending on the particle size.

Table 2. Differences in cytokine production between similar nanoparticles.

Cytokine	Types of Particles	P Value
RANTES	LP-GOs and BP-GOs, 50 μg mL^{-1}	0.0438
Eotaxin	LP-GOs, 5 and 50 μg mL^{-1}	0.0220
HGF	LP-GOs, 5 and 50 μg mL^{-1}	0.0438
	LP-GOs and BP-GOs, 50 μg mL^{-1}	0.0184
M-CSF	BP-GOs, 5 and 50 μg mL^{-1}	0.0262

4. Discussion

4.1. Monocytes Viability

Previously, we investigated the 24-hour effects of P-GO nanoparticles on human peripheral blood monocytes [11]. Despite using a different method to assess viability (trypan blue staining), no significant changes in cell viability were observed, regardless of the type of nanoparticles. Therefore, it can be concluded that these nanoparticles do not have a negative impact on human monocytes, both during short-term and long-term cultivation.

Cytotoxicity studies on monocytes are usually performed using the monocytic leukemia cell line (THP-1). In 2023 it was established that reduced GO showed toxicity to THP-1 cells at concentrations greater than 62.5 mg mL^{-1} after 24 hours and greater than 125 mg mL^{-1} after 48 hours of exposure [20]. It has been shown that GO without functionalization can decrease cell viability [21]. It appears that the pegylation of nanoparticles helps to maintain the viability of monocytes. Overall, the data we present supports this trend.

It should be emphasized that the presence of statistically significant differences compared to the negative control alone cannot determine the presence or absence of cytotoxicity. In addition, the signal in cells exposed to the

test compound or nanoparticles should be at least 20% lower than that in untreated control. A dose-dependent reduction in signal should also be observed, and the results should be reproducible [22].

Taking these facts into account, P-GO nanoparticles may be cytotoxic to monocytes with increasing concentration.

4.2. Lactate Dehydrogenase Activity

It is known that the lactate dehydrogenase (LDH) enzyme catalyzes the conversion of pyruvic acid to lactic acid and NADH to NAD+ [23]. LDH, located in the cytoplasm, plays an important role in glycolysis. When cells are damaged or their membrane permeability changes, LDH leaks into the extracellular medium. Thus, an increase in LDH activity indicates cytotoxic effects of the nanomaterial.

It has been found that graphene oxide did not cause significant LDH release from the human breast cancer cell line, cells of the retinal pigment epithelium, and stromal cells from bone marrow [24–26]. However, an increase in LDH release has been observed in Leydig and Sertoli cells, glioblastoma, ovarian cancer, monocytic leukemia, embryonic kidneys, rat myocardium, and mouse kidneys [24, 27–32].

In 2021, a meta-analysis was performed to assess the toxic effects of graphene-based materials on various parameters, including lactate dehydrogenase (LDH) activity. Among the graphene-related characteristics, the importance of the features affecting LDH release was ranked in ascending order as follows: oxidation state - diameter of nanoparticles - exposure dose - surface modification - detection method - organ type [33]. In our research, the role of PEG type, particles' size and concentration were established. LP-GOb nanoparticles led to LDH leakage. It is likely that this type of particle could cause direct mechanical damage to the monocyte membrane resulting in LDH release.

Cytokine Profile

The scheme of the influence of pegylated graphene oxide nanoparticles on the cytokine profile of human monocytes is presented in Figure 4.
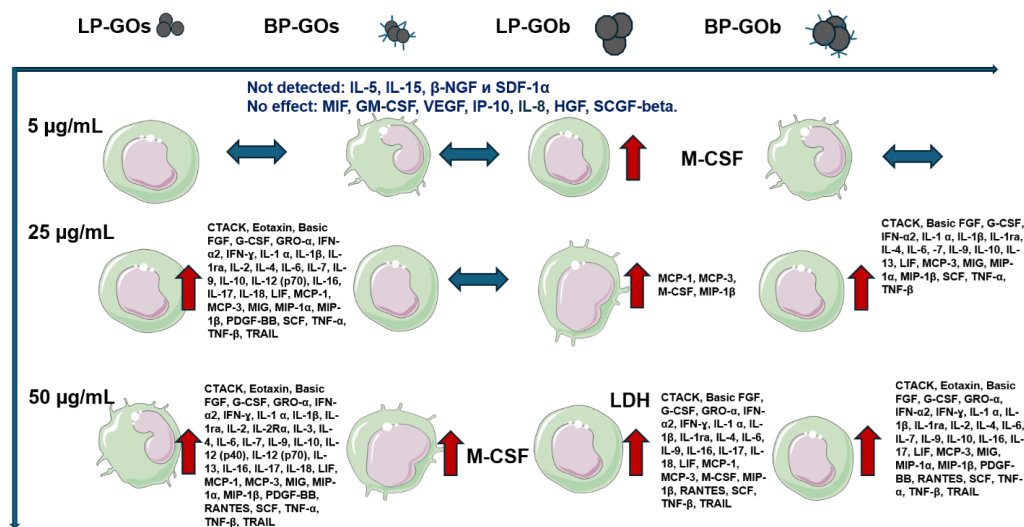
Figure 4. Summary diagram of P-GO nanoparticles' influence on the cytokine profile of monocytes.

In our study, we found that low concentrations of P-GO nanoparticles had virtually no effect on cytokine expression, with the exception of M-CSF. However, 25 and 50 µg mL^{-1} of P-GO nanoparticles significantly amplified the synthesis of various chemokines, growth factors, proinflammatory and anti-inflammatory cytokines. This indicates that higher concentrations of P-GO nanoparticles can effectively modulate the immune response by increasing cytokine production in human monocytes.

One of the primary mechanisms by which nanomaterials exert their cytotoxic effects is through the induction

of inflammation [34]. In 2017, Luo et al. established that peritoneal macrophages internalize PEGylated graphene oxide nanoparticles, which then trigger the release of pro-inflammatory cytokines by these cells [35]. A similar effect was observed with nanodiamonds, which are capable of penetrating lysosomal membranes, leading to the formation of an inflammasome [36, 37].

The literature indicates that graphene nanomaterials can induce an inflammatory response and cytokine production, potentially leading to a cytokine storm and inflammatory cell infiltration in the lungs of rats [38]. Consistent with our findings, an increase in IL-6, IL-8, IL-1β, and TNF-α pro-inflammatory cytokines expression has been noted in patients undergoing a cytokine storm. This condition is characterized by significantly elevated levels of inflammatory cytokines, including IFN-γ, MIG, IP-10, IL-6, IL-10, and IL-2Rα [39]. This aligns closely with our experimental data, although we cannot definitively characterize the situation as a cytokine storm in the context of cell culture. However, it is reasonable to assume that the high concentrations of nanoparticles we used could elicit a similar adverse reaction *in vivo.*

When studying the immunocompatibility of nanomaterials, one significant challenge is the contamination of particles with endotoxin. Monocytes are particularly responsive to lipopolysaccharides (LPS) because of their high surface levels of Toll-like receptors (TLRs), especially TLR4, which is the primary receptor for LPS [40, 41]. One study demonstrated that endotoxin-free graphene oxide did not exhibit cytotoxicity toward human macrophages and did not stimulate the synthesis of pro-inflammatory cytokines. Furthermore, this graphene oxide suppressed the release of cytokines induced by LPS [42]. At the same time, Orecchioni et al. reported non-specific activation across different cell populations, accompanied by the production of all analyzed cytokines, which is consistent with our data [43]. The results of the cytokine profile analysis suggest that if the observed responses were primarily due to stimulation with endotoxin on the particles, we would expect to see a non-specific reaction at a concentration level of 5 μg mL^{-1}, particularly given the high sensitivity of monocytes to lipopolysaccharides (LPS). However, this was not the case in our findings. The results of the LAL test of the particles used were shown in a previously published paper [13].

For further studies involving any nanomaterials, including graphene, it is essential to establish sterile synthesis protocols to produce endotoxin-free materials. The presence of endotoxin can significantly influence experimental outcomes and complicate the interpretation of results. Without clear information on particle contamination, comparing findings across different studies becomes problematic.

A comprehensive comparison of our data with the literature is complicated due to the use of particles with varying parameters. It is the combination of these parameters that ultimately determines the nature of the nanomaterial's impact on the immune system. Regarding the prediction of potential in vivo studies, the observed non-specific cytokine production is not a desirable effect; therefore, BP-GOs particles in low concentrations appear to be the most promising.

5. Conclusions

When assessing the impact of graphene oxide-PEG on the cytokine production spectrum of human monocytes, it was observed that the stimulating effect becomes more pronounced with increasing nanoparticle concentration. Specifically, 5 μg mL^{-1} of P-GO had minimal impact on cytokine production, while 25 μg mL^{-1} induced a broader range of cytokines. This effect expanded further at the highest of concentrations studied (50 μg mL^{-1}). No significant differences were noted among the various sizes of nanoparticles used in this study, but surface chemistry played a crucial role. Notably, only small nanoparticles coated with branched type of polyethylene glycol (BP-GOs) at concentrations of 5 and 25 μg mL^{-1} did not significantly affect cytokine production. However, at 50 μg mL^{-1}, they increased the production of M-CSF specifically. Overall, this modification of nanoparticles presents promising potential for developing graphene-based pharmacological agents. Importantly, PEGylated graphene oxide nanoparticles did not modulate the production of several key cytokines, such as MIF, GM-CSF, VEGF, IP-10, IL-8, HGF, and SCGF-beta by human monocytes in vitro.

Nanoparticles have been shown to induce human monocytes to produce a broad spectrum of cytokines, including proinflammatory IL-6, IL-17, IL-1α, TNF-α, IL-1β, IL-18, IL-16, TNF-β, IFN-γ, anti-inflammatory IL-10, IL-4, IL-13, IL-1ra, regulatory IL-2, G-CSF, GM-CSF, IL-3, IL-5, IL-12 (p40), IL-12 (p70), M-CSF; chemokines MIP-1α, MCP-3, CTACK, RANTES, SDF-1α, Eotaxin, MIG, MCP-1, GRO-α, MIP-1β; growth factors LIF, PDGF-BB, SCF, Basic FGF, and TRAIL.

However, these nanoparticles did not modulate the production of several other factors such as MIF, GM-CSF, VEGF, IP-10, IL-8, HGF, and SCGF-beta. Importantly, our study is the first to demonstrate that PEGylated graphene oxide nanoparticles stimulate the production of less common factors such as CTACK, Basic FGF, GRO-α, LIF, SCGF-beta, MCP-3, SCF, MIG, and TRAIL by human peripheral blood monocytes.

In summary, we can conclude that the impact of PEGylated graphene oxide nanoparticles on the properties of human monocytes is affected by several important factors, including concentration, size, and the type of PEGylation applied to the particles.

Author Contributions

Conceptualization, Z.S.A. and R.M.S.; methodology, Z.S.A. and T.V.P.; formal analysis, U.D.I.; investigation, R.M.B., S.K.Y., and U.D.I.; writing—original draft preparation, U.D.I.; writing—review and editing, T.V.P. and Z.S.A.; supervision, Z.S.A.; project administration, Z.S.A.; funding acquisition, Z.S.A. and R.M.S. All authors have read and agreed to the published version of the manuscript.

Funding

Institutional Review Board Statement

The research was carried out in accordance with the WMA Declaration of Helsinki 2000 and the Protocol of the Council of Europe Convention on Human Rights and Biomedicine 1999. Approval for the experimental design was obtained from the Ethics Committee of the IEGM Ural Branch of the Russian Academy of Sciences (IRB00010009) on 30 August 2019.

Informed Consent Statement

Informed consent was obtained from all participants involved in the study.

Data Availability Statement

The datasets used and/or analyzed during the current study are available from the corresponding author on request.

Conflicts of Interest

The authors declare that there are no conflicts of interest.

Appendix A

Table A1. Properties of P-GO.

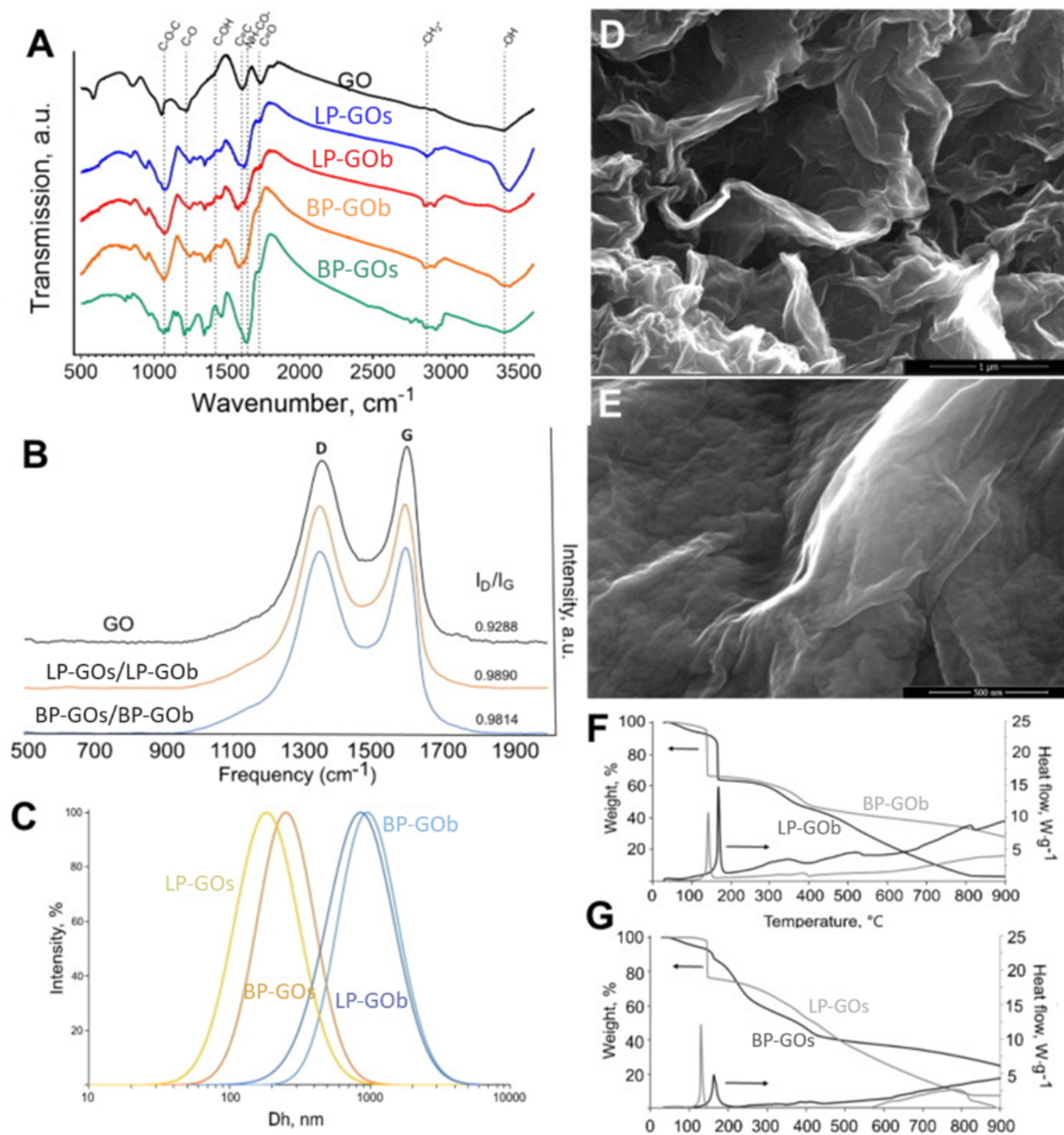|	LP-GOs	BP-GOs	LP-GOb	BP-GOb
Dh, nm [1]	184 ± 73	287 ± 52	891 ± 18	1376 ± 48
PdI	0.25 ± 0.02	0.23 ± 0.02	0.21 ± 0.02	0.30 ± 0.01
Zeta Potential, mV	−31.70 ± 1.70	−34.28 ± 0.41	−39.98 ± 1.17	−53.56 ± 1.23
PEG Coverage, wt%	17.2 ± 1.4	20.5 ± 1.8	19.4 ± 2.2	20.5 ± 1.1

[1] Dh—hydrodynamic diameter, PdI—polydispersity index.

Figure A1. Characterization of GO. (**A**)—FTIR spectra; (**B**)—Raman spectra; (**C**)—intensity-weighted size distribution determined by DLS; (**D,E**)—SEM images of GO (**D**) and BP-GOb (**E**); (**F,G**)—TGA/DSC of P-GO. Scale bars are 1 μm (**D**) and 500 nm (**E**).

Appendix B

Table A2. Cytokine and chemokine concentrations in monocyte cultures with P-GO, (n = 4), Me (Q1–Q3).

P-GO Type	Control	LP-GOs			BP-GOs			LP-GOb			BP-GOb		
P-GO Concentration, µg/mL		5	25	50	5	25	50	5	25	50	5	25	50
Inflammatory cytokines													
IFNγ	0 (0-4.9)	19.9 (17.0-30.3)	50.9 (36.8-54.10) **	53.5 (49.5-62.2) **	0 (0-13.0)	16.4 (8.8-27.3)	18.2 (12.2-35.5)	16.1 (8.4–27.5)	32.2 (20.2-54.7)	39.3 (29.4-53.7) *	17.2 (11.6-30.4)	39.34 (27.5-44.1)	46.5 (40.7-52.4) **
IL-1α	n.d.	25.3 (16.3-49.9)	265.7 (138.4-316.9) **	389.1 (285.1-443.2) ***	3.8 (0-8.9)	16.0 (10.5-22.3)	19.3 (11.6-43.9)	21.5 (11.3-27.1)	68.40 (18.2-168.0)	130.9 (40.4-275.0) *	18.8 (10.2-38.9)	165.2 (56.2-290.1) *	298.2 (144.3-384.6) **
IL-1β	2.0 (0.9-12.4)	34.1 (13.1-152.5)	1222.0 (262.8-2144.0) ***	3449 (1128.0-5183.0) ***	2.9 (1.6-12.7)	25.6 (9.0-45.4)	33.7 (6.0-122.9)	24.4 (4.6-61.9)	281.1 (19.9-818.0)	738.1 (120.0-1628.0) *	25.9 (9.4-92.5)	650.5 (88.2-1776.0) *	2592 (440.8-4660.0) ***
IL-6	86.2 (15.0-532.8)	3403 (1386-5547)	7009 (6086-7726) **	7286 (6895-7955) ***	134.9 (20.7-665.4)	1066 (263-1606)	650.1 (230.9-2707.0)	613.1 (147.1-2122)	3585.0 (718.6-6386.0)	5317 (3556-6977) *	1360 (457.9-6977)	6036 (2845-6406) *	7203 (6934-7462) **
IL-17	0.4 (0-1.1)	4.6 (2.9-7.5)	33.6 (20.0-41.6) **	50.5 (36.3-57.4) ***	1.4 (0.2-2.4)	4.6 (3.4-5.4)	4.4 (3.3-10.3)	5.4 (3.4-6.4)	13.1 (4.7-27.4)	23.6 (9.0-41.0) *	3.3 (2.6-8.2)	27.2 (9.9-43.7)	42.0 (24.2-53.1) ***
IL-18	n.d.	0 (0-3.6)	8.6 (5.1-12.1)	12.9 (11.3-15.7) **	n.d.	4.9 (1.0-5.9)	7.4 (4.2-10.3)	7.0 (1.7-14.9)	14.45 (6.6-18.6) *	13.4 (6.1-16.4)	0 (0-3.2)	11.1 (7.7-12.2)	10.5 (7.6-14.4)
TNF-α	44.7 (19.6-265.1)	844.6 (387.8-1408)	6773 (4557-8436) **	45458 (17542-48144) ***	48.1 (35.9-187.8)	359.9 (115.7-543.5)	295.7 (138.0-933.8)	423.0 (156.5-662.6)	1509 (355.9-2581)	2654 (1224-4555)	731.8 (227.1-1196)	3895 (1454-5431) *	6057 (4257-9249) **
IFNα2	n.d.	10.4 (7.9-14.6)	42.3 (32.3-48.1) **	50.6 (46.9-53.5) ***	5.3 (1.1-6.3)	10.2 (8.1-15.1)	12.7 (11.8-17.9)	11.2 (9.6-15.4)	23.3 (12.7-38.8)	32.6 (17.1-43.7) *	9.3 (2.3-15.1)	34.0 (19.3-45.0) *	45.0 (33.0-50.5) **
TNF-β	2.4 (0-7.1)	13.5 (10.4-16.9) **	45.3 (33.2-51.5) **	69.2 (61.9-85.7) ***	6.3 (6.0-11.0)	14.4 (10.6-15.7)	15.4 (12.0-18.8)	13.1 (9.3-14.2)	25.5 (11.5-38.5)	38.6 (22.0-51.8) *	(9.8-17.3)	41.3 (31.3-48.9) *	58.5 (48.5-69.5) *
IL-2Rα	n.d.	n.d.	81.4 (51.3-102.0)	110.3 (82.9-124.0) *	n.d.	n.d.	n.d.	n.d.	57.5 (36.7-71.9)	52.1 (18.5-89.9)	n.d	58.5 (22.7-87.2)	88.0 (55.0-104.5)
IL-16	56.5 (51.9-64.5)	70.7 (58.0-95.4)	215.4 (138.6-272.3) *	263.8 (202.1-295.6) **	70.0 (45.6-96.0)	77.1 (52.8-122.0)	92.9 (73.4-159.1)	80.5 (63.4-118.0)	142.9 (83.9-224.8)	179.1 (96.1-290.6) *	62.8 (47.2-98.4)	170.9 (105.6-268.7)	245.6 (152.7-294.2) **
IL-9	7.3 (1.1-11.3)	17.9 (12.6-27.8)	66.4 (47.5-68.9) **	78.4 (74.6-107.6) ***	8.1 (6.7-12.0)	17.1 (16.6-19.5)	17.1 (14.0-33.0)	18.3 (13.5-25.6)	18.3 (13.5-25.6)	36.7 (18.4-50.4) *	18.8 (12.8-27.6)	55.1 (37.5-59.0) *	81.5 (66.2-95.6) ***
MIF	547.3 (353.6-625.4)	331.1 (297.1-413.3)	867.0 (651.4-1088)	1075 (1010-1595)	375.9 (316.8-445.7)	466.5 (443.7-522.9)	525.4 (469.7-622.1)	461.3 (376.0-528.3)	634.0 (405.2-656.4)	519.2 (399.9-696.0)	285.3 (213.2-366.1)	491.7 (454-591.5)	671.4 (564.7-794.5)
IP-10	208.3 (84.8-695.2)	448.0 (101.1-1008)	341.1 (91.95-597.0)	201.0 (108.2-455.3)	192.0 (73.2-436.6)	263.0 (144.5-833.0)	277.7 (117.3-1112)	247.1 (118.9-414.8)	193.3 (94.5-479.3)	111.1 (82.2-453.1)	347.2 (189.6-754.5)	145.5 (88.0-768.7)	107.2 (74.4-199.4)
IL-8	21181 (18137-25253)	22714 (203450-24988)	22271 (21021-24390)	22805 (16939-26983)	23557 (18923-24627)	23659 (21696-26005)	23574 (22191-25181)	22521 (20127-24026)	21881 (21318-23949)	24136 (16574-25652)	20840 (18600-24471)	21014 (15378-22777)	15572 (15153-19161)

Table A2. *Cont.*

P-GO Type	Control	LP-GOs			BP-GOs			LP-GOb			BP-GOb		
P-GO Concentration, µg/mL		5	25	50	5	25	50	5	25	50	5	25	50
Antiinflammatory cytokines													
IL-4	n.d.	5.0 (4.1-7.5)	17.4 (13.5-19.1) **	20.1 (17.6-21.3) ***	1.4 (0-2.8)	4.7 (4.1-6.3)	4.7 (4.2-8.8)	4.4 (3.4-6.3)	10.4 (5.7-15.8)	14.3 (8.8-18.1) *	4.3 (2.6-7.1)	14.0 (8.5-17.1) *	17.2 (13.6-20.2) **
IL-10	0.9 (0-2.0)	37.7 (17.2-48.2)	642.3 (428.6-915.7) ***	1816 (1173-1970) ***	2.4 (0.9-3.5)	9.1 (7.9-9.6)	15.6 (9.1-21.5)	5.6 (2.3-11.0)	28.2 (7.9-77.6)	111.7 (27.5-213.7)	11.4 (7.4-18.3)	186.3 (93.5-327.8) *	416.1 (266.3-464.4) **
IL-13	n.d.	0 (0-1.5)	4.6 (3.7-5.3)	5.4 (4.3-5.8) **	n.d.	n.d.	0 (0-1.5)	0 (0-1.3)	2.8 (0.5-3.9)	3.7 (2.3-4.7)	0 (0-2.3)	3.1 (0.6-3.7)	4.4 (2.9-5.0)
TRAIL	n.d.	38.1 (20.2-119.6)	449.3 (200.2-549.3) *	578.5 (434.5-686.5) ***	0 (0-10.9)	25.2 (5.1-55.9)	35.9 (5.7-133.8)	16.3 (0-61.2)	179.6 (22.6-410.8)	337.6 (128.0-552.9) *	25.1 (5.3-94.5)	322.2 (80.3-502.2)	511.2 (256.0-627.7) **
LIF	0.3 (0-2.3)	19.8 (15.1-44.9)	186.6 (114.9-233.9) **	245.6 (189.9-276.8) ***	3.9 (1.2-12.1)	18.9 (16.3-29.3)	24.2 (18.5-50.0)	28.5 (19.8-35.6)	68.8 (28.0-141.2)	122.5 (48.5-201.4) *	17.6 (7.1-38.1)	140.8 (65.6-197.0) *	209.5 (141.0-247.8) ***
IL-1Rα	1388 (6752-3226)	8243 (5315-9729)	17856 (11938-35100) *	30084 (21871-64960) ***	2739 (1627-4535)	10521 (4964-10692)	11226 (4631-17951)	12078 (6287-19663)	18593 (10279-32921)	23753 (17855-42055) ***	10949 (5138-13120)	20313 (11872-29785) *	21647 (12014-37948) **
Regulatory cytokines, colony-stimulating factors, growth factors													
IL-2	0 (0-2.6)	10.5 (2.2-22.5)	97.8 (60.1-105.3) *	114.5 (103.0-122.7) **	n.d.	4.5 (0.8-8.1)	3.8 (0-16.6)	5.7 (1.1-8.7)	24.45 (3.6-49.4)	50.0 (18.4-74.2)	10.3 (1.8-22.2)	69.8 (26.3-91.8)	92.6 (62.3-103.1) *
IL-7	n.d.	15.8 (2.9-20.2)	40.0 (24.5-50.8) **	45.9 (34.2-53.5) ***	5.7 (0-11.4)	13.7 (11.4-19.1)	16.0 (12.6-19.1)	14.9 (3.4-17.6)	24.1 (17.0-30.7)	25.9 (17.0-34.2)	8.0 (0-22.1)	27.0 (24.1-38.9) *	33.3 (26.0-45.1) **
IL-12 (p70)	n.d.	0 (0-1.0)	1.8 (1.1-2.9) *	2.7 (2.0-3.8) *	n.d.	n.d.	0.3 (0-0.7)	n.d.	0.5 (0-1.1)	0.9 (0.5-1.5)	n.d.	1.0 (0.2-1.5)	1.5 (0.8-1.9)
VEGF	n.d.	n.d.	181.8 (0-715.7)	889.7 (588.9-1199)	n.d.	235.9 (0-569.8)	377.2 (82.5-505.7)	n.d.	0 (0-271.1)	0 (0-286.7)	n.d.	0 (0-275.8)	n.d.
M-CSF	n.d.	4.6 (3.1-19.3)	9.7 (9.2-17.5)	9.1 (8.0-10.6)	0 (0-9.5)	42.3 (13.8-62.5)	73.1 (37.8-88.3) **	46.2 (26.8-84.2)	62.2 (38.1-149.3) ***	43.0 (28.6-83.2) *	13.7 (10.1)	26.6 (12.0-62.6)	16.0 (11.7-28.4)
G-CSF	98.3 (74.2-127.9)	538.0 (414.2-671.5)	2854 (1909-4664) **	6684 (5958-10355) ***	231.4 (180.7-438.9)	606.4 (426.4-687.8)	681.9 (591.0-832.5)	620.4 (527.5-692.4)	833.0 (589.2-1654)	1285 (724.1-3841) *	455.0 (346.3-557.8)	1235 (813.4-5283) *	3241 (2305-6983) ***
SDF-1α	n.d.	n.d.	81.0 (64.8-89.9) *	93.2 (87.0-97.9) *	n.d.	n.d.	n.d.	n.d.	29.3 (0-71.3)	33.7 (0-70.7)	n.d.	37.8 (0-79.4)	78.7 (62.5-96.3)
Basic FGF	n.d.	33.5 (26.8-47.5)	109.0 (82.4-117.9) **	126.3 (111.8-131.7) ***	0 (0-20.1)	36.2 (27.7-41.2)	38.1 (32.2-53.7)	36.4 (28.6-41.3)	58.8 (34.8-96.2)	81.2 (46.1-114.0) *	28.5 (7.0-39.1)	89.8 (53.9-114.1) *	113.8 (88.4-129.0) **
IL-3	n.d.	0 (0-0.9)	7.3 (5.0-9.6)	9.9 (7.8-10.2) *	n.d.	n.d.	0 (0-1.4)	n.d.	2.4 (0-5.8)	4.5 (0.5-8.1)	0 (0-0.7)	5.1 (1.8-7.8)	8.1 (4.4-9.5)
IL-12 (p40)	0 (0-14.0)	13.5 (0-28.5)	152.0 (90.5-167.5)	207.4 (154.8-237.4) *	n.d.	0 (0-14.0)	9.3 (0-36.9)	n.d.	49.5 (0-109.8)	94.2 (33.5-159.7)	9.3 (0-21.8)	111.1 (19.3-173.4)	159.6 (99.3-197.7)
PDGF-BB	0 (0-11.3)	23.5 (5.1-48.2)	235.1 (129.7-280.0) **	278.7 (224.5-320.3) **	0 (0-11.3)	26.2 (22.1-32.4)	20.7 (20.7-48.8)	(5.9-33.7)	87.6 (33.1-192.2)	144.8 (63.1-212.0)	28.9 (5.2-60.6)	164.3 (62.2-232.8)	235.0 (143.4-304.0) **

Table A2. *Cont.*

P-GO Type / P-GO Concentration, µg/mL	Control	LP-GOs			BP-GOs			LP-GOb			BP-GOb		
		5	25	50	5	25	50	5	25	50	5	25	50
SCF	0.8 (0-2.1)	8.3 (7.1-15.8)	55.9 (40.0-68.6) **	76.4 (62.2-83.4) ***	3.5 (1.7-4.3)	7.0 (6.7-12.4)	8.8 (7.1-19.1)	7.6 (5.9-11.5)	24.3 (9.1-47.1)	37.3 (17.9-56.0) *	6.7 (6.1 (14.5)	40.7 (20.3-56.8) *	56.5 (40.5-66.2) **
GM-CSF	n.d.	n.d.	8.5 (5.5-23.4)	35.4 (10.9-115.6)	n.d.	n.d.	n.d.	n.d.	0 (0-5.2)	4.5 (0-38.8)	n.d.	7.3 (0-76.7)	112.4 (17.4-192.6)
VEGF	n.d.	n.d.	181.8 (0-715.7)	889.7 (588.9-1199)	n.d.	235.9 (0-569.8)	377.2 (82.5-505.7)	n.d.	0 (0-271.1)	0 (0-286.7)	n.d.	0 (0-275.8)	n.d.
HGF	190.0 (119.7-723.1)	90.3 (58.2-189.9)	262.0 (176.1-337.5)	336.4 (266.9-411.7)	96.8 (66.3-276.4)	63.2 (58.4-184.3)	82.1 (56.3-182.5)	87.6 (69.4-219.6)	148.7 (62.2-269.7)	194.9 (92.3-295.8)	92.9 (73.1-273.0)	211.4 (101.3-287.5)	291.3 (184.6-346.7)
SCGF-beta	593.8 (149.6-866.8)	459.4 (197.1-742.3)	1277 (934.9-1773)	1808 (1507-2395)	271.6 (124.6-445.4)	280.7 (216.4-326.2)	341.3 (258.2-456.6)	643.8 (274.3-792.4)	834.1 (781.4-886.8)	896.7 (279.3-1340)	534.4 (312.5-669.7)	980.0 (467.4-669.7)	1031 (459.3-1469)
IL-5							n.d.						
IL-15							n.d.						
β-NGF							n.d.						
Chemokines													
GRO-α	0 (0-6073)	8453 (4395-11390)	27630 (10565-50615) **	59755 (29004-254560) ***	0 (0-3611)	3516 (1199-9058)	2761 (1691-11586)	1659 (397.2-7501)	12354 (3448-24131)	15701 (12341-42731)	3984 (1774-8037)	12262 (9874-20784)	17825 (14656-22748) *
MCP-1	226.0 (56.4-1258)	5039 (1169-10290)	13625 (4158-14727) *	13980 (12608-15038) **	805.2 (517.3-1206)	9649 (7899-11678)	9276 (8115-12667)	1302 (1107-1782)	10786 (8752-12658) *	12127 (11345-13841) *	2404 (1216-6910)	1100 (1016-2559)	7898 (1645-12418)
MIP-1α	15.5 (11.4-24.4)	91.3 (61.4-95.5)	805.8 (560.2-1028) **	740.9 (477.4-1029) **	38.2 (30.4-71.6)	164.4 (76.6-210.1)	178.0 (106.3-283.9)	149.0 (106.8-250.1)	343.6 (161.4-460.8) *	441.4 (165.5-898.3)	71.6 (58.2-80.7)	417.5 (336.6-583.5) *	975.0 (678.4-982.2) **
RANTES	17.1 (14.4-31.3)	32.8 (25.5-43.2)	153.0 (127.6-193.4)	261.1 (160.7-444.9) **	24.8 (13.0-28.4)	27.2 (15.5-36.7)	27.0 (5.6-41.7)	34.1-24.2-55.6)	74.0 (48.9-114.2)	128.6 (100.5-167.6) **	23.9 (16.5-46.5)	133.7 (97.5-173.9)	245.9 (172.6-303.4) **
MIG	n.d.	26.5 (17.6-42.9)	109.6 (81.2-122.4) **	126.6 (107.6-141.8) ***	n.d.	33.6 (20.4-37.4)	28.6 (25.9-52.9)	25.8 (16.5-35.2)	51.6 (22.9-90.5)	79.8 (43.3-110.6)	38.4 (23.7-72.2)	92.3 (61.2-121.7) *	112.0 (85.3-122.6) **
Eotaxin	n.d.	n.d.	8.8 (.7-11.5) *	13.7 (12.1-15.2) **	0.6 (0-1.5)	1.7 (0.3-3.5)	3.7 (0.8-4.6)	0 (0-1.6)	3.8 (0-7.9)	6.5 (2.4-9.4)	0 (0-1.1)	6.9 (.0-10.1)	8.2 (5.1-9.7) *
MIP-1β	137.3 (95.9-201.4)	527.0 (444.8-648.8)	10302 (8598-11808) **	12023 (10840-12766) ***	370.8 (303.5-497.4)	634.2 (567.4-764.7)	590.1 (578.1-705.5)	660.7 (578.3-785.4)	1093 (650.1-4817)	3613 (802.0-6931) *	455.2 (401.4-570.9)	6364 (1361-10709) *	12587 (10883-14293) ***
MCP-3	97.3 (40.0-324.4)	1026 (615.1-3038)	6217 (2536-6578) **	5981 (5246-6793) **	140.7 (71.5-423.2)	627.9 (208.6-1717)	516.0 (366.5-4011)	352.7 (223.5-1748)	3708 (794.6-6288) *	5505 (4593-6861) **	667.2 (248.9-2096)	5081 (2051-7102) *	5499 (3761-5719) **
CTACK	0 (0-0.3)	8.2 (3.6-22.8)	70.52 (50.8-79.3) **	76.5 (68.0-91.8) ***	0.5 (0.1-0.9)	3.0 (1.8-5.1)	3.0 (1.8-11.6)	2.7 (2.1-7.3)	16.2 (3.1-46.)	31.7 (13.1-53.5) *	4.4 (1.2-13.7)	44.4 (15.1-74.3) *	72.4 (50.0-90.0) ***
SDF-1α							n.d.						

* p ≤ 0.05; ** p ≤ 0.01; *** p ≤ 0.001; n.d.– not detected.

References

1.   Pandit, S.; Gaska, K.; Kádár, R.; et al. Graphene-Based Antimicrobial Biomedical Surfaces. *Chemphyschem* **2021**, *22*, 250–263. [CrossRef]
2.   Svadlakova, T.; Holmannova, D.; Kolackova, M.; et al. Immunotoxicity of Carbon-Based Nanomaterials, Starring Phagocytes. *Int. J. Mol. Sci.* **2022**, *23*, 8889. [CrossRef]
3.   Wang, H.; Gu, W.; Xiao, N.; et al. Chlorotoxin-Conjugated Graphene Oxide for Targeted Delivery of an Anticancer Drug. *Int. J. Nanomed.* **2014**, *9*, 1433–1442. [CrossRef]
4.   Zhang, Y.; Nayak, T.R.; Hong, H.; et al. Graphene: A Versatile Nanoplatform for Biomedical Applications. *Nanoscale* **2012**, *4*, 3833–3842. [CrossRef]
5.   Kim, J.; Park, S.J.; Min, D.H. Emerging Approaches for Graphene Oxide Biosensor. *Anal. Chem.* **2017**, *89*, 232–248. [CrossRef]
6.   Lin, J.; Chen, X.; Huang, P. Graphene-Based Nanomaterials for Bioimaging. *Adv. Drug Deliv. Rev.* **2016**, *105*, 242–254. [CrossRef]
7.   Asadi, M.; Ghorbani, S.H.; Mahdavian, L.; et al. Graphene-Based Hybrid Composites for Cancer Diagnostic and Therapy. *J. Transl. Med.* **2024**, *22*, 611. [CrossRef]
8.   Hoseini-Ghahfarokhi, M.; Mirkiani, S.; Mozaffari, N.; et al. Applications of Graphene and Graphene Oxide in Smart Drug/Gene Delivery: Is the World Still Flat? *Int. J. Nanomed.* **2020**, *15*, 9469–9496. [CrossRef]
9.   Park, E.J.; Lee, S.J.; Lee, K.; et al. Pulmonary Persistence of Graphene Nanoplatelets May Disturb Physiological and Immunological Homeostasis. *J. Appl. Toxicol.* **2017**, *37*, 296–309. [CrossRef]
10. Gustafson, H.H.; Holt-Casper, D.; Grainger, D.W.; et al. Nanoparticle Uptake: The Phagocyte Problem. *Nano Today* **2015**, *10*, 487–510. [CrossRef]
11. Makharza, S.; Cirillo, G.; Bachmatiuk, A.; et al. Graphene Oxide-Based Drug Delivery Vehicles: Functionalization, Characterization, and Cytotoxicity Evaluation. *J. Nanopart. Res.* **2013**, *15*, 2099. [CrossRef]
12. Singh, D.P.; Herrera, C.E.; Singh, B.; et al. Graphene Oxide: An Efficient Material and Recent Approach for Biotechnological and Biomedical Applications. *Mater. Sci. Eng. C Mater. Biol. Appl.* **2018**, *86*, 173–197. [CrossRef]
13. Khramtsov, P.; Bochkova, M.; Timganova, V.; et al. Interaction of Graphene Oxide Modified with Linear and Branched PEG with Monocytes Isolated from Human Blood. *Nanomaterials* **2021**, *12*, 126. [CrossRef]
14. Uzhviyuk, S.; Bochkova, M.; Timganova, V.; et al. PEGylated Graphene Oxide and Monocyte Metabolism. *AIP Conf. Proc.* **2024**, *2924*, 050005. [CrossRef]
15. Mukherjee, S.P.; Bottini, M.; Fadeel, B. Graphene and the Immune System: A Romance of Many Dimensions. *Front. Immunol.* **2017**, *8*, 673. [CrossRef]
16. Tang, J.; Cheng, W.; Gao, J.; et al. Occupational Exposure to Carbon Black Nanoparticles Increases Inflammatory Vascular Disease Risk: An Implication of an ex Vivo Biosensor Assay. *Part. Fibre Toxicol.* **2020**, *17*. [CrossRef]
17. Di Ianni, E.; Møller, P.; Vogel, U.B.; et al. Pro-Inflammatory Response and Genotoxicity Caused by Clay and Graphene Nanomaterials in A549 and THP-1 Cells. *Mutat. Res. Genet. Toxicol. Environ. Mutagen.* **2021**, *872*, 503405. [CrossRef]
18. Kinaret, P.A.S.; Scala, G.; Federico, A.; et al. Carbon Nanomaterials Promote M1/M2 Macrophage Activation. *Small* **2020**, *16*, 1907609. [CrossRef]
19. Aventaggiato, M.; Valentini, F.; Caissutti, D.; et al. Biological Effects of Small Sized Graphene Oxide Nanosheets on Human Leukocytes. *Biomedicines* **2024**, *12*, 256. [CrossRef]
20. Cebadero-Dominguez, Ó.; Casas-Rodríguez, A.; Puerto, M.; et al. In Vitro Safety Assessment of Reduced Graphene Oxide in Human Monocytes and T Cells. *Environ. Res.* **2023**, *232*, 116356. [CrossRef]
21. Yan, J.; Chen, L.; Huang, C.C.; et al. Consecutive Evaluation of Graphene Oxide and Reduced Graphene Oxide Nanoplatelets Immunotoxicity on Monocytes. *Colloids Surf. B. Biointerfaces* **2017**, *153*, 300–309. [CrossRef]
22. Longhin, E.M.; El Yamani, N.; Rundén-Pran, E.; et al. The Alamar Blue Assay in the Context of Safety Testing of Nanomaterials. *Front. Toxicol.* **2022**, *4*, 981701. [CrossRef]
23. Feng, Y.; Xiong, Y.; Qiao, T.; et al. Lactate Dehydrogenase A: A Key Player in Carcinogenesis and Potential Target in Cancer Therapy. *Cancer Med.* **2018**, *7*, 6124–6136. [CrossRef]
24. Kregielewski, K.; Fraczek, W.; Grodzik, M. Graphene Oxide Enhanced Cisplatin Cytotoxic Effect in Glioblastoma and Cervical Cancer. *Molecules* **2023**, *28*, 6253. [CrossRef]
25. Yan, L.; Wang, Y.; Xu, X.; et al. Can Graphene Oxide Cause Damage to Eyesight? *Chem. Res. Toxicol.* **2012**, *25*, 1265–1270. [CrossRef]
26. Wójcik, B.; Zawadzka, K.; Sawosz, E.; et al. Cell Line-Dependent Adhesion and Inhibition of Proliferation on

Carbon-Based Nanofilms. *Nanotechnol. Sci. Appl.* **2023**, *16*, 41–57. [CrossRef]

27. Gurunathan, S.; Kang, M.H.; Jeyaraj, M.; et al. Differential Cytotoxicity of Different Sizes of Graphene Oxide Nanoparticles in Leydig (TM3) and Sertoli (TM4) Cells. *Nanomaterials* **2019**, *9*, 139. [CrossRef]

28. Choi, Y.J.; Kim, E.; Han, J.; et al. A Novel Biomolecule-Mediated Reduction of Graphene Oxide: A Multifunctional Anti-Cancer Agent. *Molecules* **2016**, *21*, 375. [CrossRef]

29. Gurunathan, S.; Kang, M.H.; Jeyaraj, M.; et al. Differential Immunomodulatory Effect of Graphene Oxide and Vanillin-Functionalized Graphene Oxide Nanoparticles in Human Acute Monocytic Leukemia Cell Line (THP-1). *Int. J. Mol. Sci.* **2019**, *20*, 247. [CrossRef]

30. Gurunathan, S.; Arsalan Iqbal, M.; Qasim, M.; et al. Evaluation of Graphene Oxide Induced Cellular Toxicity and Transcriptome Analysis in Human Embryonic Kidney Cells. *Nanomaterials* **2019**, *9*, 969. [CrossRef]

31. Zhang, J.; Cao, H.Y.; Wang, J.Q.; et al. Graphene Oxide and Reduced Graphene Oxide Exhibit Cardiotoxicity Through the Regulation of Lipid Peroxidation, Oxidative Stress, and Mitochondrial Dysfunction. *Front. Cell Dev. Biol.* **2021**, *9*, 616888. [CrossRef]

32. Chen, W.; Wang, B.; Liang, S.; et al. Understanding the Role of the Lateral Dimensional Property of Graphene Oxide on Its Interactions with Renal Cells. *Molecules* **2022**, *27*, 7956. [CrossRef]

33. Ma, Y.; Wang, J.; Wu, J.; et al. Meta-Analysis of Cellular Toxicity for Graphene via Data-Mining the Literature and Machine Learning. *Sci. Total Environ.* **2021**, *793*, 148532. [CrossRef]

34. Farrera, C.; Fadeel, B. It Takes Two to Tango: Understanding the Interactions between Engineered Nanomaterials and the Immune System. *Eur. J. Pharm. Biopharm.* **2015**, *95*, 3–12. [CrossRef]

35. Luo, N.; Weber, J.K.; Wang, S.; et al. PEGylated Graphene Oxide Elicits Strong Immunological Responses despite Surface Passivation. *Nat. Commun.* **2017**, *8*, 14537. [CrossRef]

36. Fusco, L.; Avitabile, E.; Armuzza, V.; et al. Impact of the Surface Functionalization on Nanodiamond Biocompatibility: A Comprehensive View on Human Blood Immune Cells. *Carbon* **2020**, *160*, 390–404. [CrossRef]

37. Knötigová, P.T.; Mašek, J.; Hubatka, F.; et al. Application of Advanced Microscopic Methods to Study the Interaction of Carboxylated Fluorescent Nanodiamonds with Membrane Structures in THP-1 Cells: Activation of Inflammasome NLRP3 as the Result of Lysosome Destabilization. *Mol. Pharm.* **2019**, *16*, 3441–3451. [CrossRef]

38. Kong, C.; Chen, J.; Li, P.; et al. Respiratory Toxicology of Graphene-Based Nanomaterials: A Review. *Toxics* **2024**, *12*, 82. [CrossRef]

39. Fajgenbaum, D.C.; June, C.H. Cytokine Storm. *N. Engl. J. Med.* **2020**, *383*, 2255–2273. [CrossRef]

40. Vallhov, H.; Qin, J.; Johansson, S.M.; et al. The Importance of an Endotoxin-Free Environment during the Production of Nanoparticles Used in Medical Applications. *Nano Lett.* **2006**, *6*, 1682–1686. [CrossRef]

41. Oostingh, G.J.; Casals, E.; Italiani, P.; et al. Problems and Challenges in the Development and Validation of Human Cell-Based Assays to Determine Nanoparticle-Induced Immunomodulatory Effects. *Part. Fibre Toxicol.* **2011**, *8*, 8. [CrossRef]

42. Mukherjee, S.P.; Kostarelos, K.; Fadeel, B. Cytokine Profiling of Primary Human Macrophages Exposed to Endotoxin-Free Graphene Oxide: Size-Independent NLRP3 Inflammasome Activation. *Adv. Healthc. Mater.* **2018**, *7*, 1700815. [CrossRef]

43. Orecchioni, M.; Bedognetti, D.; Newman, L.; et al. Single-Cell Mass Cytometry and Transcriptome Profiling Reveal the Impact of Graphene on Human Immune Cells. *Nat. Commun.* **2017**, *8*, 1109. [CrossRef]